A New Automated Ultrasound Quantification of Urethral Mobility for Stress Urinary Incontinence

A Feasibility Study

Kourosh Kalayeh, PhD, J. Brian Fowlkes, PhD, Bryan S. Sack, MD, Jennifer LaCross, DPT, PhD, Stephanie Daignault-Newton, MS, Payton Schmidt, MD, Haowei Tai, PhD, William W. Schultz, PhD, James A. Ashton-Miller, PhD, John O. DeLancey, MD

Article includes CME test

Supplemental material online at jultrasoundmed.org

Received November 1, 2024, from the Department of Radiology, University of Michigan, Ann Arbor, Michigan, USA (K.K., J.B.F., H.T., J.O.D.); Department of Urology, University of Michigan, Ann Arbor, Michigan, USA (K.K., B.S.S., S.D.-N.); Department of Biomedical Engineering, University of Michigan, Ann Arbor, Michigan, USA (J.B.F., J.A.A.-M.); Department of Obstetrics and Gynecology, University of Michigan, University of Michigan, Ann Arbor, Michigan, USA (J.L., P.S., J.O.D.); and Department of Mechanical Engineering, University of Michigan, Ann Arbor, Michigan, USA (W.W.S., J.A.A.-M.). Manuscript accepted for publication February 23, 2025.

The authors thank Sarah Richardson for her help in volunteer recruitment and clinical coordination. This research was supported by NIH grant NIH 5 RC2 DK122379-05. Co-author Jennifer LaCross was supported by grants NIH 5TL1DK136046-03 and NIH 5U2CDK129445-03.

There are no conflicts of interest to be reported for this publication.

Address correspondence to Kourosh Kalayeh, Department of Radiology, University of Michigan, Ann Arbor, MI, USA.

E-mail: kouroshm@umich.edu

Abbreviations

CLAHE, contrast limited adaptive histogram equalization; DICOM, Digital Imaging and Communications in Medicine; ICC, Intraclass correlation coefficient; IRB, Institutional Review Board; ROI, region of interest; SUI, stress urinary incontinence; TPUS, transperineal ultrasound

doi:10.1002/jum.16676

This is an open access article under the terms of the Creative Commons Attribution-NonCommercial-NoDerivs License, which permits use and distribution in any medium, provided the original work is properly cited, the use is non-commercial and no modifications or adaptations are made.

Objectives—Stress urinary incontinence (SUI) is a prevalent condition that can significantly affect quality of life. Urethral mobility is an important factor in SUI and transperineal ultrasound (TPUS) imaging can provide clear visualization of this movement; however, its quantification has been limited. An automated system to track and quantify urethral movement could provide richer information and reduce inter-observer effects on measurements.

Methods—As proof-of-concept for technique development, we used TPUS cine loops obtained on commercial scanners (GE Healthcare and Philips Healthcare) from consented research volunteers. We developed the tracking software based on fundamental concepts from computer vision, specifically corner detection and optical flow-based tracking algorithms. In doing so we account for inadvertent probe movements by using the symphysis pubis as a reference coordinate system.

Results—The system successfully tracks the motion of the urethra during Valsalva maneuvers. It accurately captures and quantifies complex movements, including directional shifts, rotations, displacement vectors of different structures, and the trajectory of motion. These measurements are corrected for any probe movement. We demonstrated the system's efficiency and reliability in near real-time analysis across various ultrasound platforms and video formats. The intraclass correlation coefficients exceeded 0.89 and 0.5 for intra- and inter-rater reliability, respectively.

Conclusions—By providing detailed, objective measurements of urogenital movement, this approach has potential to advance the understanding, diagnosis and treatment of SUI, which in turn, can help tailor more effective treatment strategies. This methodology paper confirms the feasibility of automated quantification of urethral mobility.

Key Words—computer vision; female pelvic floor; image processing; pelvic floor muscle contraction; stress urinary incontinence; transperineal ultrasound; urogenital mobility

Stress urinary incontinence (SUI) is characterized by involuntary urine leakage during activities that increase intra-abdominal pressure, such as coughing, sneezing, or exercising.[1] This condition predominantly impacts women[2] and significantly affects their quality of life, impacting social,

© 2025 The Author(s). *Journal of Ultrasound in Medicine* published by Wiley Periodicals LLC on behalf of American Institute of Ultrasound in Medicine.

psychological, occupational, and sexual well-being.[3] SUI primary causal factors are poor urethral function and defective support of the urethra and bladder neck.[4]

Understanding and quantifying the dynamics of pelvic floor and urethral support is important in SUI management. Abnormal urethral support has been recognized as a crucial factor in etiology and treatment outcomes of SUI.[5] For example, among women with poor urethral function, tape insertion surgeries had a success rate of 100% for those with a hypermobile urethra, while only a 67% success for those with a hypomobile urethra.[6] This highlights the significance of urethral support in both the cause and treatment of SUI.

Transperineal ultrasound (TPUS) imaging presents a non-invasive technique that allows real-time visualization of pelvic floor and bladder neck movements.[7] Despite its advantages, TPUS effectiveness in SUI evaluation is limited by the subjective nature of manual image interpretation and observer variability. Most established techniques to measure urethral support require time-consuming manual analysis and are not widely used in clinical practice.[8] Additionally, significant variation still exists in the literature concerning which aspects of urethral support should be measured.[9] Typically, a resting image is compared with an image at maximal excursion, leaving intermediate dynamic processes unassessed.[10–12] Previous attempts at frame-by-frame analysis for capturing these dynamics, based on edge extraction algorithms,[13] have been too cumbersome for practical use and have not been adopted. Additionally, subtle but potentially critical phenomena—like pelvic muscle activation in anticipation of a cough, which can be observed in TPUS—have not been studied due to lack of techniques for analysis. These challenges, coupled with the limited understanding of normal pelvic floor function, often lead to inefficient treatment strategies, which highlight the need for more objective and automated tools in SUI management.

Given the rapid development of computer vision in medical image assessment over the last decade, its application in evaluating pelvic floor functionality emerges as particularly promising. This technology has the potential for not only assessing standard parameters but also discovering movements previously unnoticed. By integrating computer vision with TPUS, this study aims to develop a real-time methodology for capturing the dynamic movements of the pelvic floor structures.

This feasibility study demonstrates a novel approach that allows analysis across different ultrasound platforms and video formats, eliminating the need for specialized personnel, reducing costs and enhancing accessibility. It also provides immediate feedback, allowing clinicians to verify if the observed movements align with qualitative expectations. These features demonstrate the potential for widespread adoption and represent a significant step forward in enhancing our understanding and management of SUI, thereby improving patient outcomes and the overall quality of care.

Methods

A schematic illustration of the female pelvic floor, depicting various urogenital structures, along with a corresponding typical sagittal TPUS B-mode image, is shown in Figure 1 (the corresponding cine loop is shown in online supplemental Video 1). As shown in the figure, and as will be further detailed, the ultrasound probe is positioned on the perineum in a mid-sagittal orientation for imaging. A critical aspect to consider is the motion artifact introduced by the movement of the ultrasound probe relative to the pelvis during the examination. This motion, which is necessary to prevent the probe from restricting natural movement of the urethra, lacks diagnostic value and must be decoupled from the structural displacements and deformations. To address this challenge, in line with previous research,[14] we use the symphysis pubis as a stationary reference point due to its rigid structure. Therefore, as will be shown, we describe urethral motion in relation to a coordinate system attached to the pubis. This, in turn, enables us to compare movements of adjacent structures and allows for the contextual registration of these movements.

Experimental Protocol

Ten female consented volunteers, aged 20–76 years with a mean age (± standard deviation) of 41.4 (±15.8) years, were recruited in an ongoing Institutional Review Board (IRB) approved study (IRBMED ID: HUM00181787). The study's exclusion criteria included any history of prolapse, current

cancer treatment, chronic urinary tract infections, organ transplantation, prior pelvic area injuries or accidents, and pregnancy or childbirth within the last 3 months. After confirming the absence of a urinary tract infection based on urinalysis and symptoms, B-mode TPUS imaging was performed in the lithotomy position using clinical scanners: GE Healthcare (General Electric Healthcare, Wauwatosa, WI, USA) Voluson® E10 with a curvilinear C2-9-D probe or Philips (Philips Healthcare, Bothell, WA, USA) EPIQ® 5 W with a linear eL 18-4 probe. The frame rate was set to the maximum possible rate (typically, 30 Hz), which depends on other scanning parameters such as depth, field of view, and frequency. The imaging plane and depth were picked such that the clearest images of the bladder, urethra and pubis could be obtained, with the plane centered and adjusted to anticipate and accommodate motion within the imaging area. The remaining scanning parameters (eg, frequency, mechanical index, and gain) were set for optimum image quality and on a case-by-case basis. An example of TPUS image is shown in Figure 1.

Prior to the imaging session, volunteers were instructed to void. Subsequently, for optimal imaging conditions, their bladder was filled to an approximate volume of 300 mL with saline using the Laborie Aquarius® XT urodynamic system (Laborie Medical Technologies Corp., Portsmouth, NH, USA), consisting of T-DOC® 7-Fr dual lumen catheter (CAT880), a peristaltic pump and pump tubing (TUB500). The filling was done at a rate of 30 mL/min. It might be important to note that this bladder filling procedure was not necessary for the specific analyses presented in this study and was conducted as part of the IRB approved study.

The ultrasound probe was encased in a cover (Trojan Condoms, Church & Dwight Company, Ewing Township, NJ, USA) filled with coupling gel (EcoVue Ultrasound Gel, A Division of HR® Pharmaceuticals, Inc., York, PA, USA). Additional gel was applied over the cover before positioning it on the perineum in a midsagittal orientation, ensuring sufficient skin contact to maintain the location and orientation of the urogenital structures without causing distortion. During imaging, volunteers were instructed to perform a Valsalva maneuver on command. These processes were conducted by an Obstetric and Gynecology specialist with more than 40 years practice at the University of Michigan (JOD).

The TPUS cine loops were stored with Digital Imaging and Communications in Medicine (DICOM) standard format for offline analysis. Pydicom[15] open source Python library was used to access and read the DICOM files.

Figure 1. Schematic representation (left) and typical transperineal B-mode ultrasound image (right) of the female pelvic floor. S (superior), I (inferior), P (posterior), and A (anterior) are showing anatomical directions.

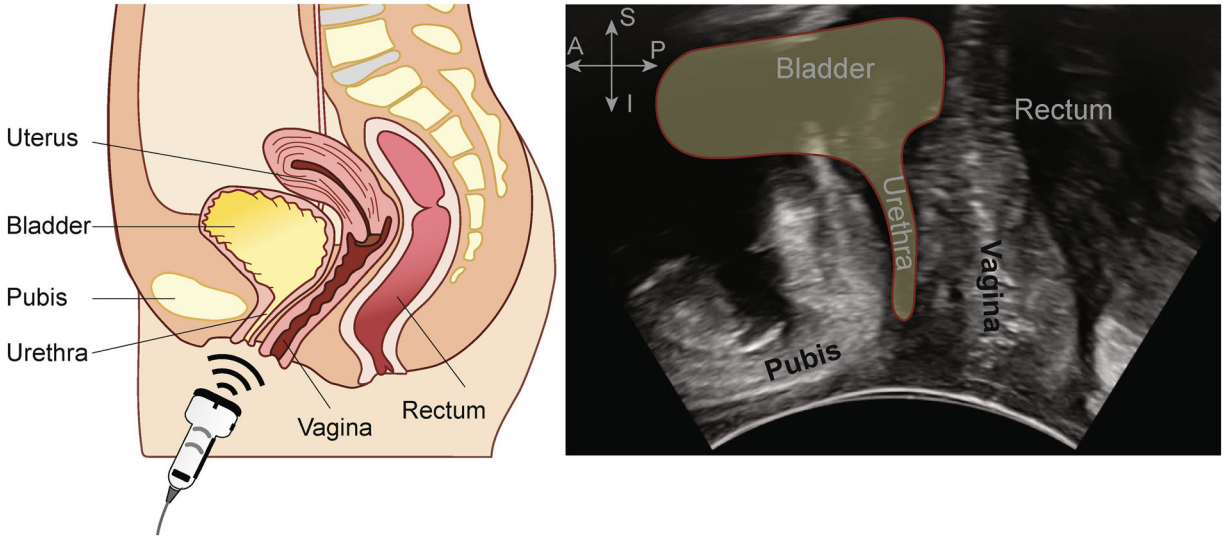


Image Processing

The image processing steps for tracking and quantifying urethral mobility in TPUS cine loops are summarized in the flowchart of Figure 2. As outlined, the procedure begins with sequentially reading each frame from the cine loops, followed by preprocessing, designating regions of interest (ROIs), identifying salient features suitable for optical flow tracking, tracking the motion by following these features points, and ultimately quantifying the motion. Python programming language and the OpenCV open source computer vision and machine learning software library was used.[16] Additionally, for scientific computation, plotting and statistical analysis, Numpy,[17] Scipy,[18] and Matplotlib[19] Python open-source libraries were used (the specific versions of the used software packages are provided in Appendix A).

Image Preprocessing

In the preprocessing step, each frame from the TPUS cine loop is initially converted to grayscale. This process converts the image data to a single gray channel, significantly simplifying subsequent processing steps while retaining essential information for our analysis. Following the grayscale conversion, contrast limited adaptive histogram equalization (CLAHE) is applied to enhance image contrast. CLAHE is particularly effective in improving the visibility of features in TPUS imaging by normalizing the brightness and increasing the contrast of the images.[20] The specific parameters for CLAHE were fine-tuned for this application (these are detailed in Appendix B). An example of the preprocessed image after grayscale conversion and CLAHE histogram equalization is shown in Figure 3.

Feature Detection

An optical flow tracking algorithm is used to follow salient feature points in the image and track motion. These feature points are obtained with the goodFeaturesToTrack algorithm from OpenCV. This algorithm is based on "corner" detection[21] and identifies regions in the image with large variation in intensity in all directions. It is based on the idea of maximizing the intensity variation function $E(u,v)$, over shifts (u,v):

$$E(u,v) = \sum_{x,y} w(x,y)(I(x+u,y+v) - I(x,y))^2, \qquad (1)$$

where $I(x,y)$ represents the intensity of the image at pixel (x,y), and $w(x,y)$ is a window function applied around the center pixel. The algorithm essentially identifies points where the minimum eigenvalue of the structure tensor of pixel intensity $I(x,y)$ is maximized, indicating significant intensity variation in all directions.[22] In OpenCV's goodFeaturesToTrack, a Gaussian window function is used to weight the pixels.[16]

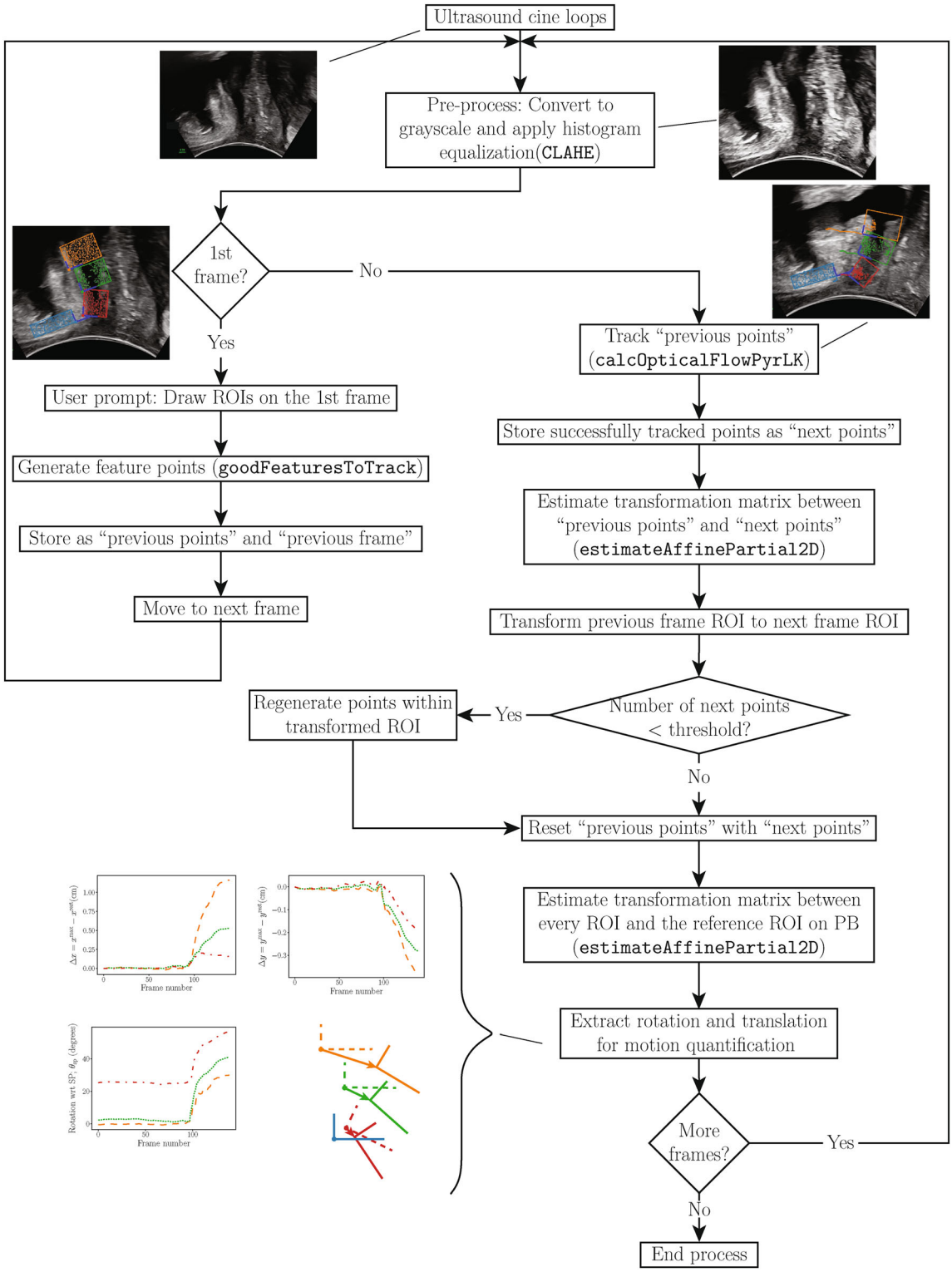
In this study, at the first frame, the user is prompted to manually draw the desired number of rectangular ROIs. Rectangular ROIs are selected for their simplicity in maintaining a consistent Cartesian coordinate system and ease in calculating angles. The reference ROI should be placed on the pubis, aligned with its long axis. The reference coordinate system $(x-y)$, essential for quantifying urethral mobility kinematics, is placed on the lower-right vertex of this ROI as shown in Figure 4, which follows the pubis based on tracking. The same figure shows the detected feature points for each ROI. In this example, the urethra is manually segmented into three rectangular ROIs: proximal to the bladder, mid-urethra, and distal to the bladder. The detailed parameters for goodFeaturesToTrack are given in Appendix B.

Motion Tracking

The feature points identified in the previous step are tracked between successive frames (i to $i+1$) using the Lucas-Kanade method,[23] a specific optical flow algorithm implemented via calcOpticalFlowPyrLK function in OpenCV (see Appendix C for its detailed arguments). Optical flow algorithms analyze the pattern of apparent motion of image objects between two consecutive frames. This method is based on two key assumptions:

1. Brightness constancy assumption: Pixel intensities of an object remain consistent between consecutive frames. This assumption asserts that the intensity $I(x,y,t)$ of a pixel at (x,y) at time t is the same as its intensity at the new position $(x+dx,y+dy)$ in the next frame at time $t+dt$:

Figure 2. Flowchart of the ultrasound image processing algorithm developed in this study for quantifying urethral mobility.



$$I(x,y,t) = I(x+dx, y+dy, t+dt). \quad (2)$$

2. Spatial coherence assumption: Neighboring pixels exhibit similar motion. This assumption allows the method to solve for the optical flow by considering a small window of pixels around each feature point.

Under these assumptions, the optical flow equation can be derived as follows:

$$\frac{\partial I}{\partial x}\frac{\partial x}{\partial t} + \frac{\partial I}{\partial y}\frac{\partial y}{\partial t} + \frac{\partial I}{\partial t} = 0 \quad (3)$$

The Lucas-Kanade method solves this equation for the displacements (dx, dy) by minimizing the sum of squared errors over a window of pixels.[23]

In the context of our study, where frame-by-frame motion is relatively small, these assumptions are generally valid. This makes the Lucas-Kanade method an appropriate choice for tracking the motion of feature points across successive frames.

Geometric Transformation and Motion Quantification

The successfully tracked points from previous step are used to estimate the geometric transformation matrix between frames i and $i+1$. In this specific application, we use a similarity transformation, which is a subset of affine transformation. The similarity transformation matrix is given by,

$$\boldsymbol{M} = \begin{bmatrix} s\cos\theta & -s\sin\theta & t_x \\ s\sin\theta & s\cos\theta & t_y \end{bmatrix}. \quad (4)$$

This transformation has four degrees of freedom; two translation (t_x, t_y), one rotation (θ) and one scaling factor (s). A similarity transformation matrix maintains the shape of an object, preserving the angles between vectors. OpenCV estimateAffinePartial2D computes the transformation matrix between two consecutive frames. This matrix, is then applied to transform the ROIs (ie, applied on their vertices), and consequently, the urogenital structures that they represent (urethra, in this case) from the previous frame to the next. This transformation matrix is used to quantify motion of urethra, and map out its trajectory during the motion.

As shown in the flowchart of Figure 2, an additional step ensures the number of successfully tracked and transformed feature points exceeds a predetermined threshold. During motion tracking, some feature points may be lost due to factors such as occlusion, or changes in tissue echogenicity due ultrasound angle-dependent backscatter. If the number of successfully tracked feature points falls below this

Figure 3. Example of preprocessed (gray converted and histogram equalized) ultrasound image. S (superior), I (inferior), P (posterior), and A (anterior) are showing anatomical directions.

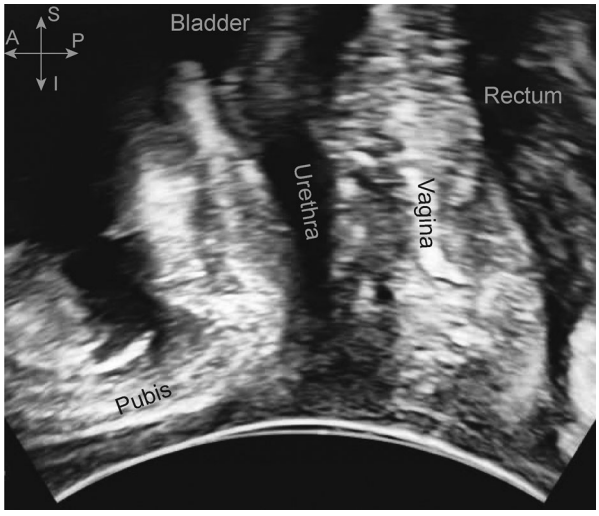
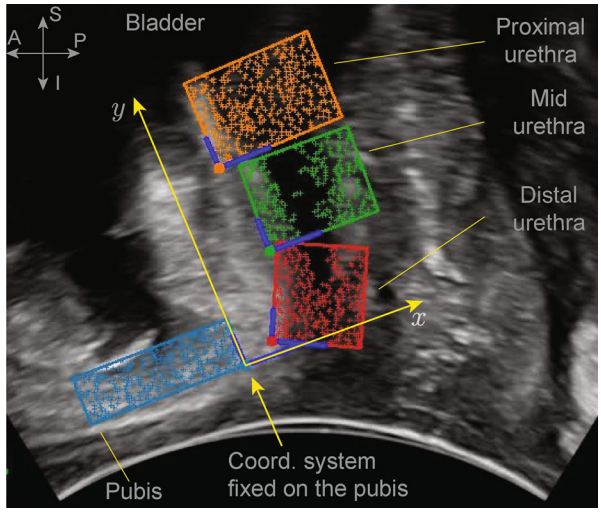


Figure 4. Selection of regions of interest (ROIs) for urethral mobility analysis with corresponding detected feature points—plus marks (+). The ROI on the pubis serves as the reference ROI.



threshold, indicating the tracking accuracy could be compromised, a new set of features is regenerated within the transformed ROIs.

The same approach determines the relative motion of the urethra with respect to the pubis. Specifically, the transformation between each ROI and the reference ROI on pubis is calculated. The rotation component of each transformation matrix indicates the rotation of its corresponding ROI relative to the pubis. The translation components represent the displacements.

Intra- and Inter-Reliability

To evaluate the reliability and repeatability of the developed software, a series of intra- and inter-rater analysis were conducted. These analyses involved computing intraclass correlation coefficients (ICCs) for a set of metrics based on examinations of the 10 volunteers included in this study. The metrics for reliability analysis were comprised of displacement components $(\Delta x, \Delta y)$, motion vector magnitude and direction $(|\boldsymbol{d}|, \phi)$ and ROIs rotation $(\Delta\theta)$ at maximum excursion. For intra-rater reliability, co-author KK independently analyzed blinded videos on three separate occasions over the span of 1 month. To assess inter-rater reliability, co-authors, JL and JOD each performed an independent analysis. The same Obstetric and Gynecology specialist co-author, responsible for TPUS imaging (JOD), trained all individuals involved in the analysis.

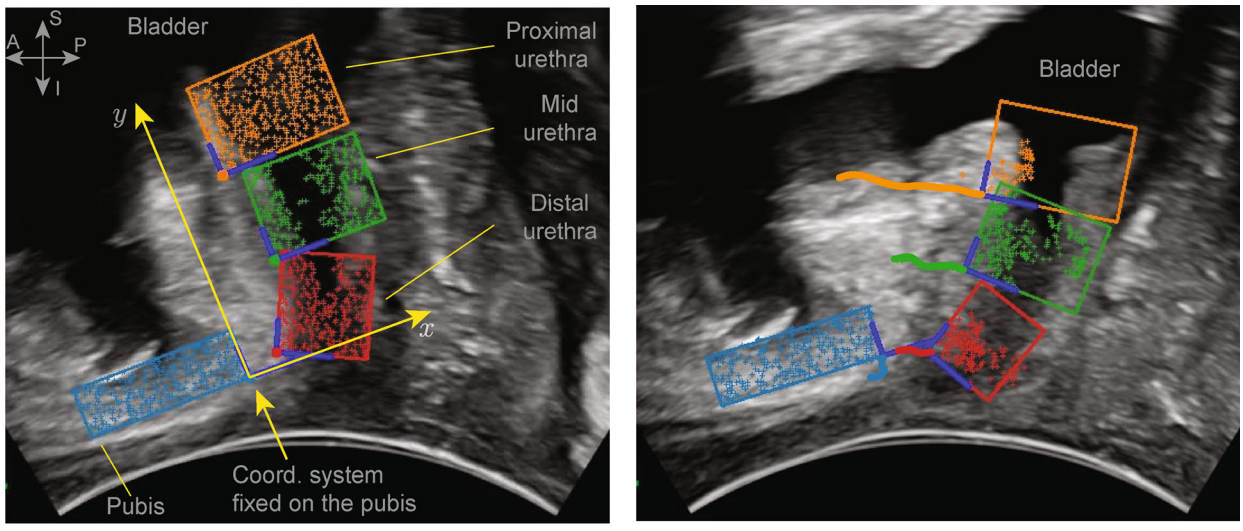
Results

Following the same example that has been used thus far, Figure 5 shows tracking of the urethral motion during the Valsalva maneuver. Specifically, the pelvic floor at the rest state and maximum excursion is shown in Figure 5, A and B, respectively. Consistent with the literature,[13] the urethral movement during this maneuver is in an inferior-posterior direction that is, in $+x$ and $-y$ directions, where x and y are coordinate system on the pubis (see Figure 4). The corresponding videos are shown in online supplemental Videos 2 and 3, with and without feature points, respectively. For each urethral segment, the traveled distance, its direction and rotation are determined.

Trajectory of Motion

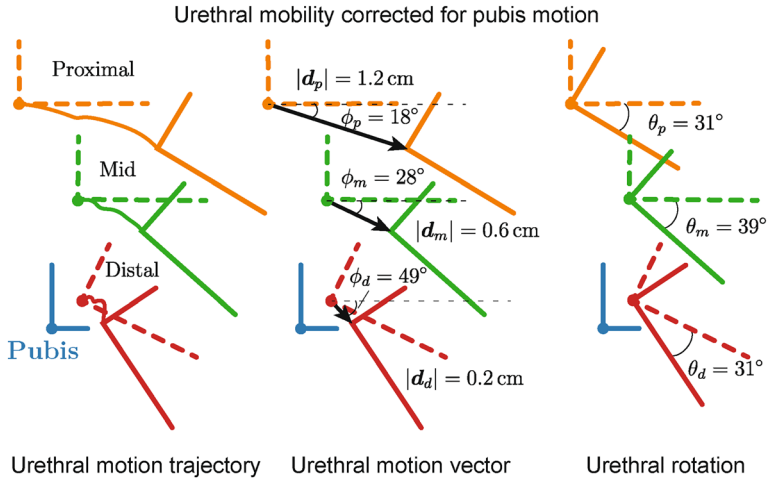
The trajectory of motion for each urethral segment is mapped out in left panel of Figure 6. In this figure, the pubis remains stationary, and the urethral

Figure 5. Example of pelvic floor tracking during Valsalva. Pelvic floor (**A**) in a rest state and (**B**) at maximum excursion is shown. While here the urethra and pubis are being tracked, the ROIs can be placed anywhere on the ultrasound image.



A B

Figure 6. Urethral mobility analysis with pubis motion correction. Motion of the proximal, mid and distal urethra segments, from rest (dashed lines) to maximum excursion (solid lines), is shown. The figure is obtained for Valsalva maneuver and corresponds to the ultrasound images of Figures 4 and 5.



motion trajectory is corrected for any pubis motion. The displacement vector ($\boldsymbol{d}$) for each ROI is detailed in center panel of the figure, including its magnitude ($|\boldsymbol{d}|$) and directional angle (ϕ). These vectors provide quantitative insights into the total motion of the urethra during the maneuver, highlighting the extent and direction of motion for each segment. Finally, rotation of each urethral segment with respect to its initial position is depicted in the right panel of the figure. The corresponding video, showing trajectory of motion, is shown in online supplemental Video 4.

Quantification of Urethral Mobility

The displacement components of each urethral segment in the x and y directions are shown in Figure 7, A and B, respectively. As before, x and y are parameterizing the coordinate system attached to the pubis (see Figure 4). The rotation of each urethral segment with respect to the pubis is shown in

Figure 7. Quantification of urethral mobility capturing pelvic floor dynamics during Valsalva maneuver. The displacements of urethral segments in (**A**) anterior–posterior (Δx) and (**B**) inferior–superior (Δy) directions are plotted against frame number. In quantifying the displacements, the coordinate system moving with the pubis corrects for motion artifact; $x-y$ coordinate system shown in Figure 4.

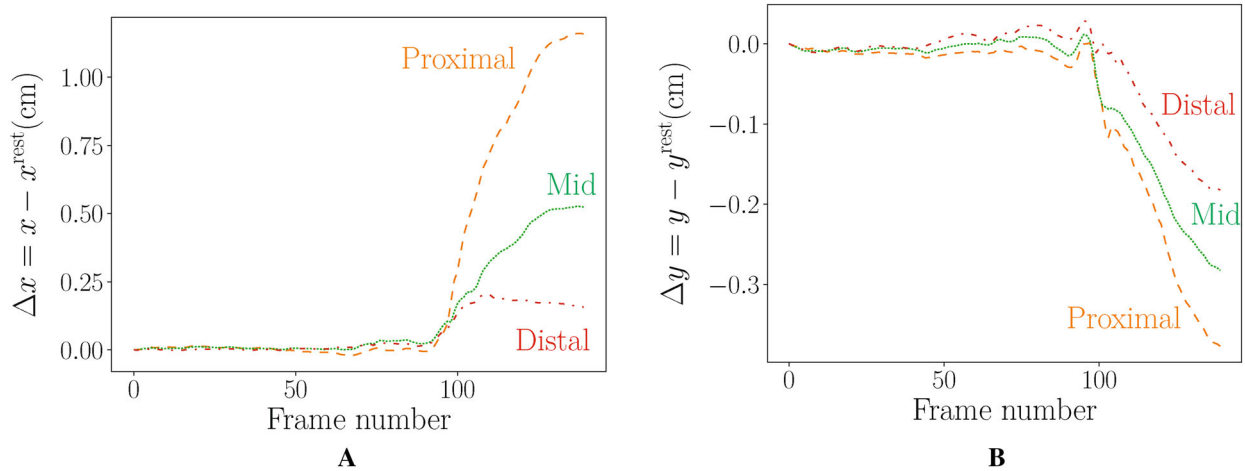


Figure 8. (**A**) Relative angle (θ) and (**B**) rotation ($\Delta\theta$) of urethral segments with respect to the pubis during Valsalva maneuver. Positive and negative numbers are indicative of clockwise and counter clockwise rotation, respectively.

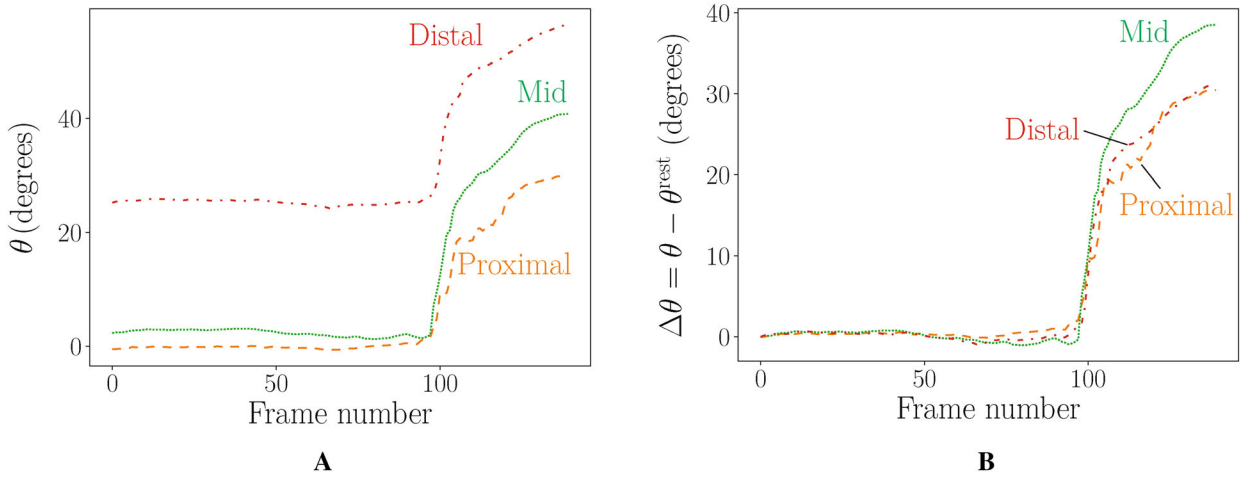
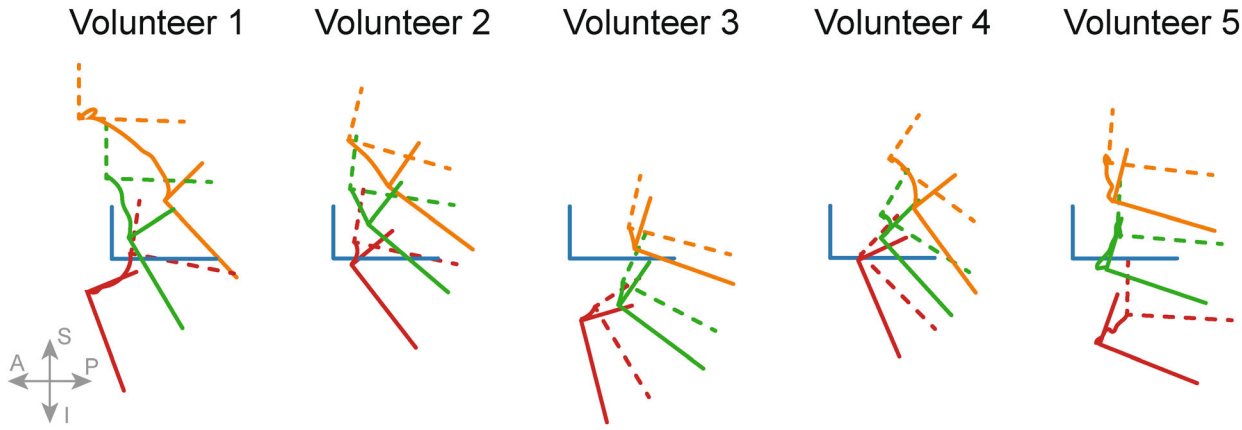


Figure 8. Specifically, the angular relationship between each urethral segment relative to the pubis, along with its change across frames is plotted in Figure 8, A and B. In doing so, the right angle bracket placed at the origin of the ROIs on the urethra is used (dark blue brackets of Figures 4 and 5). For quantifying rotation, positive and negative values denote clockwise and counter clockwise rotations, respectively. Consistent with Figures 5 and 6, the quantification results reveal that as intra-abdominal pressure increases during the Valsalva maneuver, the urethra predominantly moves in an inferior posterior direction.

The results of Figures 7 and 8 emphasize that the urethral motion is not uniform. The proximal urethra, including the bladder neck, experiences the largest displacement in the x- and y-directions, followed by mid and distal urethra. These patterns indicate a urethral "kinking" or "bending" phenomenon. This kinking phenomenon is further confirmed in Figure 8, particularly in Figure 8B, which shows that the mid-urethra undergoes maximum rotation during

Figure 9. Individual variability in urethral mobility. Example of urethral mobility during Valsalva maneuver for five different volunteers. As shown, not only urethra initial position at rest state differ between individuals but the total motion and the path that the urethra travels are different as well.



the maneuver. This observation of varying rotation and displacement across urethral segments has the potential to provide valuable insights into the biomechanical behavior of the urethra under conditions of stress.

Individual Variability in Urethral Mobility

As an example and a proof of concept, Figure 9 compares urethral mobility of five different volunteers during the Valsalva maneuver (selected from 10 total subjects to avoid clutter). The trajectories of motion for the proximal, mid and distal urethral segments, from the rest state to maximum excursion, are shown. Similar to Figure 6, the pubis in these figures remain stationary and the displayed urethral motion accounts for any concurrent pubis motion.

In the figure, the pubis of all volunteers are aligned for better visualization and to facilitate comparison. The figure describes and compares the differences between the trajectories of different volunteers qualitatively. As shown, not only is the initial position (the rest state) of the urethra distinct for each volunteer, but the paths that it traverses, the magnitude it attains, and the direction and degrees of motion also exhibit significant inter-subject variability.

Intra- and Inter-Reliability

The ICCs for intra- and inter-rater reliability across each urethral segment are detailed in Table 1. These results highlight the method's high reproducibility, with intra-rater ICC > 0.89, indicating strong consistency in repeated analyses by the same rater. Inter-rater reliability is also predominantly high, showing a substantial agreement among raters. Nonetheless, a few metrics, particularly those associated with the distal ROI, had ICC values in the moderate range (ICC > 0.5). It is important to emphasize that the inter-rater results are based on measurements conducted by only two raters, with one rater (JL) being relatively inexperienced in TPUS imaging of the pelvic floor. Despite the moderate ICC values observed for certain metrics, these results are still considered highly correlated within a clinical context. This is particularly noteworthy given the novel nature of the methodology, the limited number of cases for rater training, and the study pioneering approach. The detail of reliability results are shown in the Figures C1 and C2.

Discussion

Urethral mobility has long been recognized as an important factor in the pathophysiology and management of SUI,[24] with surgical management typically designed to enhance urethral support.[25] A significant increase in postoperative failures among individuals

Table 1. Intra- and Inter-Reliability of the Developed Methodology in Tracking Urethra During Valsalva Maneuver

		Intra-rater reliability			Inter-rater reliability		
		ICC	**95% CI**	***P***	**ICC**	**95% CI**	***P***
Proximal	$\Delta\theta$	0.96	[0.88, 0.99]	<.01	0.90	[0.68, 0.97]	<.01
	Δx	0.98	[0.94, 0.99]	<.01	0.89	[0.65, 0.97]	<.01
	Δy	0.96	[0.88, 0.99]	<.01	0.97	[0.89, 0.99]	<.01
	ϕ	0.96	[0.90, 0.99]	<.01	0.53	[−0.07, 0.86]	.04
	$\lvert\boldsymbol{d}\rvert$	0.97	[0.91, 0.99]	<.01	0.98	[0.91, 0.99]	<.01
Mid	$\Delta\theta$	0.98	[0.96, 1.00]	<.01	0.97	[0.88, 0.99]	<.01
	Δx	0.93	[0.81, 0.98]	<.01	0.73	[0.26, 0.92]	<.01
	Δy	0.95	[0.86, 0.99]	<.01	0.95	[0.81, 0.99]	<.01
	ϕ	0.96	[0.90, 0.99]	<.01	0.92	[0.72, 0.98]	<.01
	$\lvert\boldsymbol{d}\rvert$	0.90	[0.75, 0.97]	<.01	0.77	[0.34, 0.94]	<.01
Distal	$\Delta\theta$	0.97	[0.93, 0.99]	<.01	0.95	[0.83, 0.99]	<.01
	Δx	0.90	[0.76, 0.97]	<.01	0.50	[−0.11, 0.85]	.05
	Δy	0.89	[0.73, 0.97]	<.01	0.65	[0.10, 0.90]	.01
	ϕ	0.89	[0.74, 0.97]	<.01	0.53	[−0.07, 0.86]	.04
	$\lvert\boldsymbol{d}\rvert$	0.90	[0.74, 0.97]	<.01	0.57	[−0.02, 0.87]	.03

Intraclass correlation coefficients (ICC) are computed based on transperineal ultrasound of the 10 volunteers examined in this study.

with limited urethral mobility[6] underscores the need for simple reliable techniques to quantify this mobility. While TPUS imaging provides clear visualization of urethral motion, its quantification has largely been a manual process, focusing on only a small part of the visible motion.[9] Most studies concentrated on the movement of the bladder neck,[11] while others assessed multiple points along the urethra's length.[26] Nonetheless, these approaches quantified urethral mobility by comparing a resting image with one at maximum stress, capturing only a fraction of the urethra's dynamic behavior during changes in intra-abdominal pressure. These approaches are inherently time-consuming and fail to capture the path traversed by the urethra during motion and its rotation. Additionally, they do not consider other subtle observations, such as perineal body elevation in anticipation of maneuvers like coughing, which might provide information with significant value. The Constantinou group[13] broadened the scope of analysis with much richer series of assessment by considering the full dynamic of motion during various maneuvers. Despite these significant contributions, their methodology has not gained widespread adoption, primarily due to its complexity.

A noninvasive method to quantify urethral support, combined with outcome studies on treatment plans, can enhance our understanding of the factors influencing the success of surgical interventions and pelvic floor muscle training. This approach allows researchers and physicians to more effectively link the degree of support loss to surgical outcomes. The analysis of TPUS cine loops from patients with documented outcomes, along with concurrent measurements of urethral closure function, will allow key support characteristics that correlate with treatment outcomes to be identified. Such a comprehensive assessment would enable more accurate predictions of surgical success and help tailor individualized treatment strategies for better patient outcomes. As a first step in this analysis, we developed a methodology to quantify urethral mobility by leveraging computer vision.

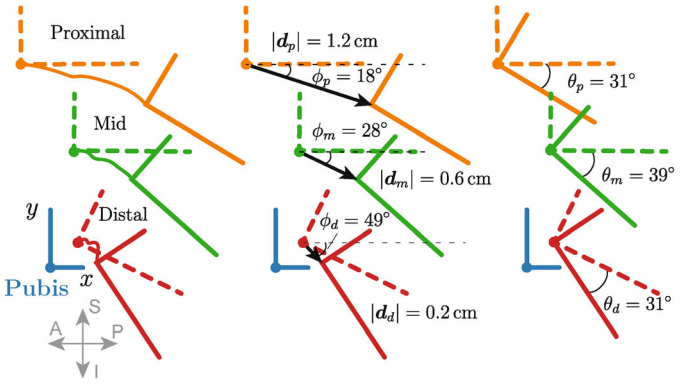
As shown in Figure 5, our methodology tracks the urethra throughout its entire dynamic range during motion, enabling a much richer series of urethral mobility assessments. This is while accounting for and separating pubis motion—which is diagnostically irrelevant—from actual urethral mobility (see Figure 6). This differentiation is vital for ensuring the accuracy of the analysis and avoiding misdiagnosis. By capturing and quantifying the trajectory, displacement vectors and rotational aspects of the urethra's motion (Figures 6–8), our method provides comprehensive diagnostic data, which can help physicians to develop effective SUI management plans. For example, our analysis can delineate and quantify the urethral "kinking" phenomenon, shedding light on its implications in the context of SUI diagnosis and management.

The robustness of our methodology, as evidenced in the intra- and inter-rater reliability section (Table 1), confirms its reliability and repeatability—essential qualities for any clinical diagnostic tool. Of course not every Valsalva is the same and, as is true with heart rate or blood pressure, one would expect variation from one time to another. This robustness of analysis of a specific maneuver allows these variations to be studied and ensures that the methodology can consistently quantify the full range of urethral mobility across different examinations, examiners, and patients.

Our study also paves the way for more nuanced comparisons between individuals. In Figure 9, for example, we demonstrated the trajectories of urethral mobility for five distinct volunteers. This comparative analysis underscores a crucial diagnostic insight that a "one size fits all" approach does not suffice in evaluating SUI. Instead, a more personalized treatment strategy, accommodating the unique motion characteristics of each individual's urethra during clinical evaluation, needs to be considered. This is consistent with our own clinical observations and those of others.[27]

In this proof-of-concept study, we propose a new methodology based on fundamental computer vision concepts to quantify pelvic floor mobility. This method can be applied to any cine loop, regardless of the TPUS machine used, and has the potential to be integrated into commercial scanners. It simplifies the evaluation of motion and broadens the scope of analysis. While we use the urethra and Valsalva maneuver as examples to explain the methodology, any other pelvic floor structures can be tracked during different maneuvers. In fact, our ongoing study analyzes the urethra, vaginal wall, bulbospongiosus, pubis, puborectalis, and anal sphincter during Valsalva, coughing, and Kegel exercises in both

Figure 10. Sample urethral mobility "report" for stress urinary incontinence evaluation. The figure presents an example report showcasing key metrics evaluating urethral mobility. The displayed metrics are illustrative and will be expanded to encompass a broader range of relevant quantities of interest in the final analysis.



	Proximal	Mid	Distal
Motion vec. mag.	1.2 cm	0.6 cm	0.2 cm
Motion vec. direction	18°	28°	49°
Rotation	31°	39°	31°
Initial x-coord.	-0.3 cm	0.2 cm	0.3 cm
Initial y-coord.	1.9 cm	1.1 cm	0.2 cm
x-disp.	1.2 cm	0.5 cm	0.2 cm
y-disp.	-0.4 cm	-0.3 cm	-0.2 cm

continent and incontinent subjects. The analysis requires only the placement of ROIs, after which a multitude of parameters are extracted in seconds, making it highly efficient and clinically applicable. Immediate feedback allows clinicians to verify motion fidelity. By eliminating the need for specialized personnel and enabling the tracking of multiple pelvic floor structures, this approach has significant potential for widespread adoption. This study demonstrates that near real-time automated quantification of pelvic floor kinematics is feasible, enabling analyses previously not possible and leading to a new diagnostic paradigm for SUI.

Vision, Next Steps, and Limitations

Our vision for this innovative technique in analyzing pelvic floor mobility is to summarize the diagnostic information into a comprehensive "report" format that physicians can readily use to evaluate urinary incontinence. An illustrative example of such a report summary is presented in Figure 10. These reports have the potential to aid physicians in stratifying patients, effectively determining who would most benefit from each type of surgical or non-surgical intervention. This ability to differentiate is crucial for developing personalized management plans tailored to individual patient needs. Future studies, linking treatment outcomes to specific parameters, can identify the most predictive factors and determine their cutoffs. These studies help understand the normal range of urethral movement, the impact of surgical interventions, and treatment outcomes. This ensures reports not only summarize data but also guide clinical decision-making. They provide reference ranges that clinicians can use to make informed treatment decisions and recommendations.

It is important to recognize current limitations and areas for future research. We have not yet examined the timing of muscle activation, which might be of clinical importance. In this study and at the methodology development stage, the focus was on urethral mobility and Valsalva maneuvers; however, evaluation of cough and pelvic muscle contraction are feasible as well and remain the topic of our ongoing research. Furthermore, a wider range of conditions, including women with pelvic organ prolapse, needs to be studied. Our current analysis relies on manual selection of ROIs, which inevitably introduces some variability. A key goal for future development is to employ machine learning for segmentation of TPUS images of the pelvic floor, enabling automatic ROI selection. This would streamline the process and further reduce variability. Our analysis currently focuses only on urethral motion from rest to maximum excursion, without examining any potential hysteresis. Similarly, we have not yet quantified changes in urethral size (bladder base and neck configuration) or assessed urethral funneling during motion. These are all factors of potential significance in SUI diagnosis and management. Addressing some of these limitations remains a topic of our ongoing research.

Conclusion

This feasibility study introduces a new technique for automatically quantifying urethral mobility in TPUS, crucial for managing SUI. Our automated, machine-agnostic approach can be integrated into commercial ultrasound scanners and processes any cine loop or video file of the pelvic floor. It is the first step for studying the relationship between the dynamics of urethral closure pressure and urethral motion. Within seconds, the software tracks urethral segments relative to the pubis and generates comprehensive data of motion. The developed method enhances the precision and repeatability of urethral mobility assessment and facilitates the development of more personalized, data-driven treatment strategies.

Beyond improving diagnostic accuracy, our method offers the ability to analyze full trajectories, displacement vectors, and rotational dynamics of urethral motion—parameters that were previously difficult to quantify. This enriched dataset not only deepens our understanding of the biomechanics underlying SUI but also lays the groundwork for predictive models that can inform treatment selection. By offering objective, reproducible metrics, this approach can standardize urethral mobility assessments across clinical settings, ultimately contributing to better patient outcomes and advancing research into pelvic floor disorders.

While the urethra and Valsalva maneuver are used as examples in this study, our methodology can also be applied to other pelvic floor structures, offering broader clinical implications. This can improve treatment for stress incontinence and other pelvic conditions where motion assessment is needed.

Data Availability Statement

The data that support the findings of this study are available from the corresponding author upon reasonable request.

References

1. D'Ancona C, Haylen B, Oelke M, et al. The International Continence Society (ICS) report on the terminology for adult male lower urinary tract and pelvic floor symptoms and dysfunction. *NeurourolUrodyn* 2019; 38:433–477.
2. Lavelle J, Ellimoottil C, Kirkali Z, et al. Trends in stress urinary incontinence procedures from 2012 to 2020 from the Uda project. *J Urol* 2023; 209:e661.
3. DeLancey J. The hidden epidemic of pelvic floor dysfunction: achievable goals for improved prevention and treatment. *Am J Obstet Gynecol* 2005; 192:1488–1495.
4. DeLancey J, Trowbridge E, Miller J, et al. Stress urinary incontinence: relative importance of urethral support and urethral closure pressure. *J Urol* 2008; 179:2286–2290.
5. DeLancey JO. Structural support of the urethra as it relates to stress urinary incontinence: the Hammock hypothesis. *Am J Obstet Gynecol* 1994; 170:1713–1723.
6. Wlaźlak E, Viereck V, Kociszewski J, et al. Role of intrinsic sphincter deficiency with and without urethral Hypomobility on the outcome of tape insertion. *NeurourolUrodyn* 2017; 36:1910–1916.
7. Dong B, Shi Y, Chen Y, Liu M, Lu X, Liu Y. Perineal ultrasound to assess the urethral spatial movement in stress urinary incontinence in women. *BMC Urol* 2023; 23:44.
8. Kania P, Rafał M, Marcin K, et al. Transperineal ultrasound as a reliable tool in the assessment of membranous urethra length in radical prostatectomy patients. *Sci Rep* 2021; 11:1759. https://doi.org/10.1038/s41598-021-81397-z.
9. Jamard E, Blouet M, Thubert T, Rejano-Campo M, Fauvet R, Pizzoferrato AC. Utility of 2D-ultrasound in pelvic floor muscle contraction and bladder neck mobility assessment in women with urinary incontinence. *J Gynecol Obstet Human Reprod* 2020; 49: 101629.
10. Weinstein M, Shobeiri SA. Instrumentation and techniques for translabial and transperineal pelvic floor ultrasound. *Practical Pelvic Floor Ultrasonography*. New York: Springer New York; 2014:45-67.
11. Li Y, Geng J, Tan C, Tang J, Yang X. Diagnosis and classification of female stress urinary incontinence by transperineal two-dimensional ultrasound. *Technol Health Care* 2017; 25:859–866.
12. Falah-Hassani K, Reeves J, Shiri R, Hickling D, McLean L. The pathophysiology of stress urinary incontinence: a systematic review and meta-analysis. *Int Urogynecol J* 2021; 32:501–552.
13. Peng Q, Jones R, Constantinou C. 2D ultrasound image processing in identifying responses of urogenital structures to pelvic floor muscle activity. *Ann Biomed Eng* 2006; 34:477–493.
14. Schaer G, Koechli O, Schuessler B, Haller U. Perineal ultrasound for evaluating the bladder neck in urinary stress incontinence. *Obstet Gynecol* 1995; 85:220–224.
15. Mason D, scaramallion, mrbean-bremen, et al. Pydicom/Pydicom: Pydicom v2.4.4. 2023.
16. Bradski G. The OpenCV library. Dr. Dobb's Journal of Software Tools. 2000.
17. Harris CR, Millman KJ, van der Walt SJ, et al. Array programming with NumPy. *Nature* 2020; 585:357–362.

18. Virtanen P, Gommers R, Oliphant T, et al. SciPy 1.0: fundamental algorithms for scientific computing in python. *Nat Methods* 2020; 17:261–272.
19. Hunter JD. Matplotlib: a 2D graphics environment. *Comput Sci Eng* 2007; 9:90–95.
20. Zuiderveld K. Contrast limited adaptive histogram equalization. *Graphics Gems*. Amsterdam, Netherlands: Elsevier; 1994.
21. Harris C, Stephens M. A Combined Corner and Edge Detector: Procedings of the Alvey Vision Conference, 1988. Alvey Vision Club; 1988.
22. Shi J, Tomasi C. Good Features to Track: Proceedings of IEEE Conference on Computer Vision and Pattern Recognition CVPR-94. IEEE Computer Society Press; 1994.
23. Lucas BD, Kanade T. An iterative image registration technique with an application to stereo vision. Paper presented at: Proceedings of the 7th International Joint Conference on Artificial Intelligence (IJCAI), Vol. 2, 1981; Vancouver, BC, Canada.
24. DeLancey JO. Why do women have stress urinary incontinence. *NeurourolUrodyn* 2010; 29(Suppl 1):S13–S17.
25. Rovner E, Wein A. Treatment options for stress urinary incontinence. *Rev Urol* 2004; 6(Suppl 3):S29–S47.
26. Ling C, Shek K, Gillor M, Caudwell-Hall J, Dietz H. Is location of urethral kinking a confounder of association between urethral closure pressure and stress urinary incontinence. *Ultrasound Obstet Gynecol* 2021; 57:488–492.
27. Roberts K, Mahajan S. Management of urgency and mixed urinary incontinence. *Clin Obstet Gynecol* 2021; 64:306–313.

Appendix A

Open-Source Software Packages Version

Python 3.11.9
matplotlib==3.8.2
numpy==1.26.2
opencv-contrib-python-rolling==5.0.0.20221015
pandas==2.1.4
pydicom==2.4.4
scipy==1.11.4

Appendix B

Detailed Parameters for Image Processing

B.1. CLAHE Histogram Equalization Parameters

clipLimit = 3
tileGridSize = (8, 8)

B.2. Shi-Tomasi Corner Detection Parameters

maxCorners = 50000
qualityLevel = 0.001
minDistance = 0.1
blockSize = 3

B.3. Lucas-Kanade Optical Flow Parameters

winSize=(31, 31)
maxLevel=11
criteria=(cv2.TERM_CRITERIA_EPS
| cv2.TERM_CRITERIA_COUNT, 50, 0.05)

Appendix C

Intra- and Inter-Rater Reliability Example

Figure C1. Intra-rater reliability example for one volunteer. The mean and standard error for every metric considered for the reliability analysis are plotted for $n = 3$ independent measurements of one individual (co-author KK). The raw data points are presented as circles.

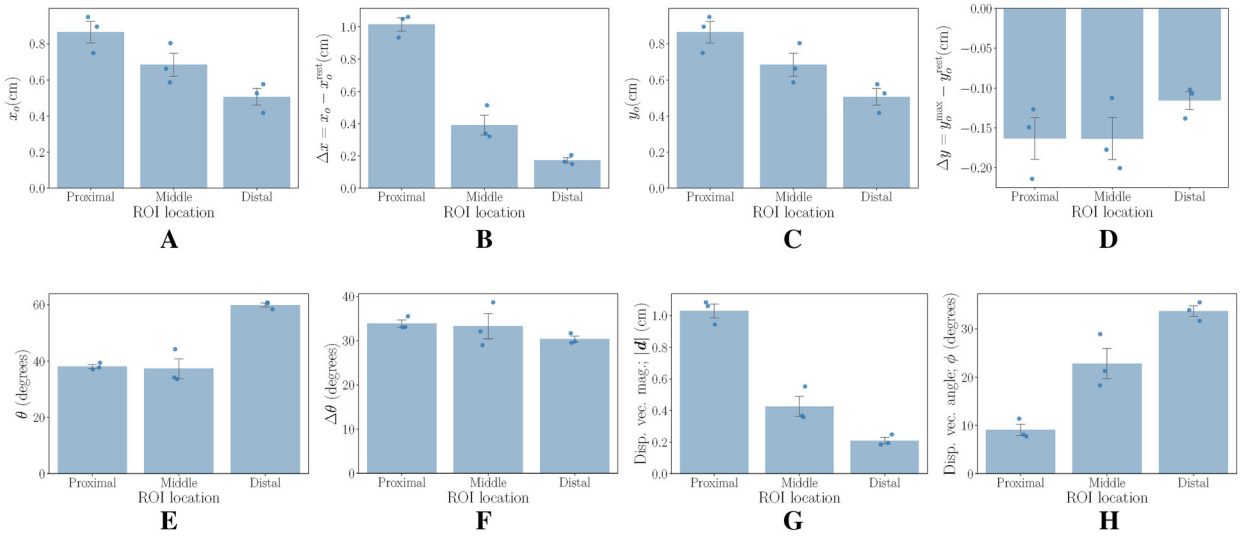


Figure C2. Inter-rater reliability example for one volunteer. The mean and standard error for every metric considered for the reliability analysis are plotted for $n = 2$ independent measurements of two independent individual (co-authors JL and JOD). The raw data points are presented with circles.

